Int J Thermophys (2009) 30:1343–1356
DOI 10.1007/s10765-009-0600-8

Modeling of Influence of Gas Atmosphere and Pore-Size Distribution on the Effective Thermal Conductivity of Knudsen and Non-Knudsen Porous Materials

Khaled Raed · Ulrich Gross

Received: 10 December 2008 / Accepted: 14 May 2009 / Published online: 2 June 2009

Abstract Application of porous insulation materials in various gas atmospheres changes their effective thermal conductivity due to many structural and thermal influences. One of those is the pore-size distribution of the material. In this paper a study of the influence and modeling of the modification of the effective thermal conductivity of various materials is presented by exchanging the gas atmosphere. For this purpose 11 different materials with various pore-size distributions are investigated. The experimental work included thermal conductivity measurements along with an analysis of the porous structure. Two additional important effects of thermal accommodation and radiation will be clearly identified as caused by the exchange of the filling gas. Modeling the gas thermal conductivity for different polydisperse systems is carried out based on kinetic theory and the Knudsen effect of rarefaction of the gas in a wide range of the Knudsen number. Development of the single pore model of the gas thermal conductivity to a new predictive model with an exponential parameter gives good agreement with the experimental results.

Keywords Gas thermal conductivity · Knudsen effect · Pore-size distribution · Porous media

List of Symbols

λ Thermal conductivity
Ψ Porosity

K. Raed (✉) · U. Gross
Institute of Thermal Engineering, Technische Universität Bergakademie Freiberg,
09599 Freiberg, Germany
e-mail: raed@iwtt.tu-freiberg.de

U. Gross (✉)
e-mail: gross@iwtt.tu-freiberg.de

α	Accommodation coefficient
Λ	Mean free path
γ	Ratio of heat capacity
ζ	Exponential parameter
C_v	Isochoric specific heat
Kn	Knudsen number
T	Temperature
P	Pressure
R	Universal gas constant
CDF	Cumulative distribution function

Subscripts

eff	Effective
CM	Continuum regime
TR	Transition regime
FM	Free-molecule regime

1 Introduction

Industrial application of thermal insulations in furnaces and similar high-temperature facilities with various gas atmospheres requires formulations of effective thermal conductivity modifications by changing the gas atmosphere. Heat transfer through such highly porous insulation materials is governed by the coupled processes of conduction through a solid matrix and filling gas and also by radiation. This implies that an exchange of the gas atmosphere in the facility causes a change of filling gas properties and consequently a modification of the effective thermal conductivity of the porous materials. A large number of mathematical models, available from the literature, can be used to estimate the effective thermal conductivity of porous materials, describing basically the contribution of conduction through the two phases (gas, solid). However, application of several of those models to estimate the effective thermal conductivity modifications by exchanging the gas atmosphere, has proved to be successful for the case of materials with macro-scaled pores. However, they fail regularly when the pores are micro- and nano-scaled. This has been demonstrated in a previous paper presented at the 17th European conference on thermophysical properties [1]. One of the main reasons is the kind of modeling used for the gas thermal conductivity with a pore size distributed in the micro- and nano-range.

The kinetic theory of gases used to estimate thermophysical properties of gases shows good agreement with measured results, e.g., for the gas thermal conductivity [2] within the limits of applicability. However, gases in rarefied regimes have different behavior than in the free regime. We have presented in previous work [3] the two theories of Knudsen and Smoluchowski which used to calculate heat transfer in rarefied gases. Kaganer [4] used the temperature jump theory developed by Smoluchowski for modeling the gas thermal conductivity in insulation materials under vac-

uum conditions. This model has often been used by many researchers to estimate the gas thermal conductivity in porous materials, in general [3]. Cunnington and Tien [5] tested Kaganer's model, and they showed good agreement with their experimental results. However, the test was done only for microsphere insulations. From their results, it is shown that by exchanging the gas atmosphere from nitrogen to helium, at atmospheric pressure and ambient temperature (300 K), increases the effective thermal conductivity by $0.12\,\mathrm{W}\cdot\mathrm{m}^{-1}\cdot\mathrm{K}^{-1}$. Actually, this is equal to the difference between the bulk thermal conductivities of the two gases, i.e., the Knudsen effect is not present in the material [3].

Harper and El Sahrigi [6] found a different behavior for the effective thermal conductivity of some foods and also for foam materials by exchanging the gas atmosphere. They used an empirical model to estimate the gas thermal conductivity with an empirical constant depending on the particular gas and also on the type of porous material. Madzhidov et al. [7] developed an equation to estimate the modification of the effective thermal conductivity of granulated aluminum oxide by exchanging the gas atmosphere and increasing the temperature, whereas that equation is more suitable for the high thermal conductivity of solids, e.g., of metals. Furthermore, investigations of the influence of the gas atmosphere on the thermal conductivity of porous materials were carried out by Keshock [8], in an effort to simulate the effective thermal conductivity of elastomeric materials in a Martian atmosphere. However, no theoretical advance was reported covering the heat transfer through porous media and their structure. Zeng et al. [9,10] have developed a new model to estimate the gas thermal conductivity, as they noticed erroneous predictions by Kaganer's model in estimating the gas thermal conductivity in nano-materials (Aerogel). In spite of the fact that the model considered the pore-size distribution, it is more limited to the structure of Aerogel material and it has been tested only at reduced gas pressures. This paper presents further progress to develop a predictive model for the thermal conductivity of rarefied gases in micro- and nano-materials, based on kinetic theory and by considering the pore-size distribution and accommodation coefficient effects.

2 Experiment

2.1 Thermal-Conductivity Measurements

The effective thermal conductivity is measured by using the steady-state radial heat flow method [11]. The apparatus allows an exchange of the gas atmosphere while keeping the sample in position. The effective thermal conductivity has been measured in various gas atmospheres (krypton, argon, nitrogen, and helium). Before this, the chamber has been regularly evacuated twice and filled with the next gas, to ensure a pure gas environment in the facility. The procedure for measuring the thermal conductivity of a certain material always starts with a gas which has the lowest thermal conductivity. For example, from the four aforementioned gases, krypton has the lowest thermal conductivity. Even if a residue of the gas remained in the sample after exchanging the gas atmosphere, the impact on the measurements will be small. The uncertainty of the measured effective thermal conductivities was estimated to be within 5 %.

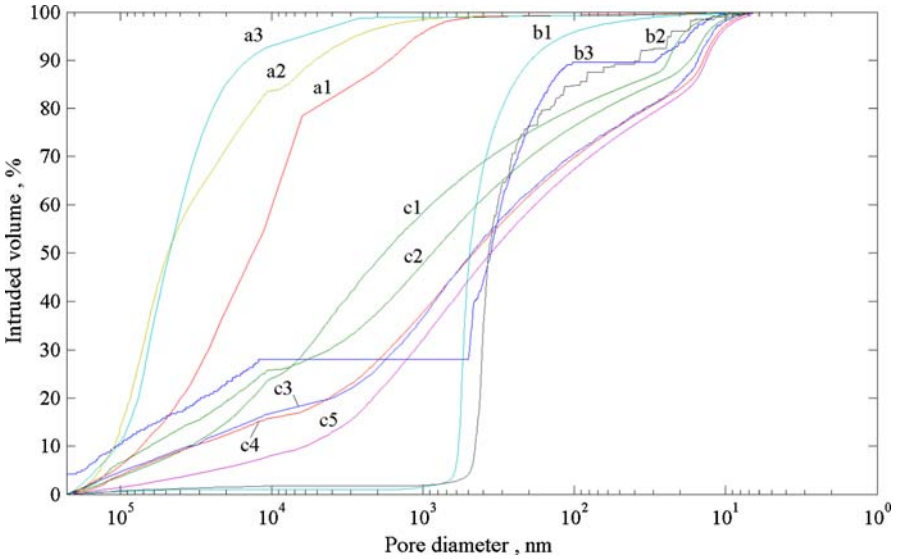

Fig. 1 Pore-size distribution of all samples

2.2 Samples

Hollow cylindrical samples (with 60 mm, 12 mm, and 60 mm as the length and inner and outer diameters, respectively) were prepared from 11 different ceramic materials which are commonly used for high-temperature insulation up to 1000 °C. The selected samples have different compositions, which are assumed to have only indirect influence on our investigations of effective thermal conductivity modifications when exposed to various gas atmospheres. The materials have a wide range of bulk densities ($217\,\mathrm{kg}\cdot\mathrm{m}^{-3} < \rho < 1{,}000\,\mathrm{kg}\cdot\mathrm{m}^{-3}$). Several samples from each material were also prepared that are suitable for mercury intrusion porosimetry for determination of the pore-size distribution. The utilized porosimeter enables detection of pore sizes scaled from micro- (200 μm) down to the nano-range (6 nm) by applying the intrusion pressure in two stages. The pore-size distribution of a material can be mathematically described as a normal distribution. We present pore-size results as the cumulative distribution function (*CDF*) varying from 0 to 1 which gives a better overview of the measured materials, see Fig. 1. A *CDF* value of 0.3 at a pore size of 10 μm, e.g., means that 30 % of the pores scale larger than 10 μm and 70 % are smaller.

Figure 1 shows the pore-size distributions of 11 samples which can be classified into three groups:

- Group (a) includes three materials, which are located in the macro-range and they are characterized by narrow pore-size distributions ranging roughly from 1 μm to 100 μm. The shape of the *CDF* curves follows the normal distribution. One of them, (a_1), is extending somewhat into the nano-range direction, i.e., this material has a larger portion of small pores than the other two (a_2 and a_3).

- Group (b) represents three materials distributed at the micro-scale and also having narrow pore-size distributions from 20 nm to 1,000 nm. The shapes of these *CDF*s correspond also to the normal distribution except (b_3) with a small portion of pores in the macro-range, i.e., it has a wide distribution from the macro- to the nano-range. Otherwise, it has a narrow distribution in each of the two ranges, namely, the macro- and nano-ranges.
- Group (c) covers five materials with wide pore-size distributions ranging from the macro- down to the nano-range. The curves extend more to the right (nano-scale) than the materials in group (b) which means that a larger portion of pores are located in the nano-range. The shape of a *CDF* for this group is described mathematically as a beta distribution.

The porosity of the materials has also been investigated, and two classes are found with group (a) ranging from 68 % to 89 % and the other two groups (b and c) with higher porosities from 90 % to 94 %.

2.3 Experimental Results

The thermal-conductivity measurements have been carried out in the temperature range from 300 °C to 700 °C exposed to various gas atmospheres, namely, krypton, argon, nitrogen, and helium. Figure 2 presents the results of thermal-conductivity measurements of two of the materials (a_3) and (b_1) plotted versus the mean temperature of the samples. Exchanging the filling gas from nitrogen to helium, i.e., to a higher thermal conductivity gas, results in an increase of the effective thermal conductivity of both materials. This is basically well known. However, the absolute and relative amounts of the increase depends on the kind of material and its pore structure as we will show

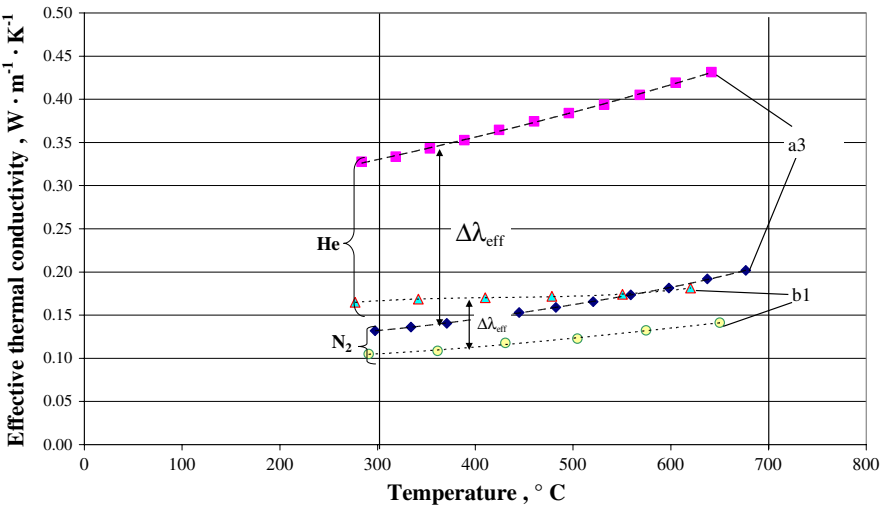

Fig. 2 Measured effective thermal conductivity of samples from two different materials in nitrogen and helium

later in this paper. As shown in Fig. 2, the increase of the thermal conductivity for the sample (a_3) at a temperature of 400 °C is about $\Delta\lambda_{\text{eff}} = 0.20\,\text{W} \cdot \text{m}^{-1} \cdot \text{K}^{-1}$ corresponding to 230 %, whereas for the sample (b_1) at the same temperature gives about $\Delta\lambda_{\text{eff}} = 0.056\,\text{W} \cdot \text{m}^{-1} \cdot \text{K}^{-1}$ corresponding to 150 %. An overview of all materials under investigation is presented in Fig. 3. All these materials have been measured at the same furnace chamber temperature (500 °C) in a nitrogen atmosphere, and the respective mean temperatures of the various samples are found to vary depending on the thermal conductivities, see Fig. 3.

3 Theoretical Background

Basically there are three different heat transfer mechanisms in porous media, namely, conduction in the solid matrix and filling gas, radiation in the solid and gas, and convection. Actually, the contribution of convection can be neglected due to the very small pore size, and the effective thermal conductivity can be written as

$$\lambda_{\text{eff}} = f(\lambda_{\text{gas}}, \lambda_{\text{solid}}, \lambda_{\text{radiation}}) \tag{1}$$

Neglecting coupling effects between the gas and solid conduction, we can formulate the effective thermal conductivity of an open pore system as

$$\lambda_{\text{eff}} = f(\lambda_{\text{solid}}, \lambda_{\text{radiation}}) + \Psi\lambda_{\text{gas}} \tag{2}$$

with Ψ as the porosity. By exchanging the gas atmosphere, we actually change the contribution of gas conduction, and the modification of the effective thermal conductivity can be written as

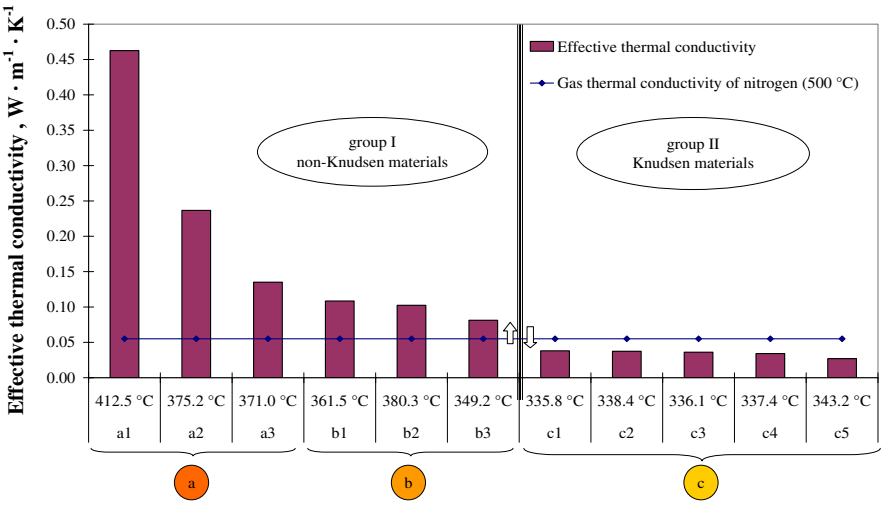

Fig. 3 Effective thermal conductivity of 11 different materials measured in nitrogen atmosphere at a constant furnace temperature of 500 °C

$$^{\text{gas}_1}\overrightarrow{\Delta\lambda_{\text{eff}}}^{\text{gas}_2} = \Psi\,\Delta\lambda_{\text{gas}} \tag{3}$$

The gas thermal conductivity will be decreased, when the pore size shifts from the macro- to nano-range caused by the Knudsen effect [3]. Along with this behavior, the effective thermal conductivity of the porous material will be decreased, and—possibly—it falls below the bulk gas thermal conductivity. As seen in Fig. 3, we have classified the investigated materials by comparing their effective thermal conductivity with the bulk thermal conductivity of nitrogen at 500 °C into group I, which will be called *non-Knudsen materials*, and group II, where the Knudsen effect is clearly noticeable, called *Knudsen materials*. The latter one corresponds to group (c), see Fig. 1, with larger portions of pores in the nano-range. The filling gas is rarefied in the pores of such systems. Independent of the porous structure, heat transfer in rarefied gases has been abundantly investigated, whereas most of the studies concern three different idealized geometries: two parallel plates, concentric cylinders, and concentric spheres [12]. The Knudsen number (Kn) is defined as the ratio of the mean free path to the characteristic length of the geometrical arrangement, and it is used for the subdivision of the gas conduction processes into three main regimes: continuum ($Kn < 0.01$), transition ($0.01 < Kn < 10$), and free-molecule regime ($Kn > 10$).

In the continuum regime (CM) the gas thermal conductivity has its bulk value as proportional to the square root of the temperature:

$$\lambda_{\text{CM}} \propto \sqrt{T} \tag{4}$$

In the free-molecule regime (FM), many models are available from the literature, and the thermal conductivity depends mainly on the kind of geometrical arrangement. For modeling heat transfer by a rarefied gas in the free-molecule regime, we have chosen the two parallel-plate model given by Kennard [13]. He treated the molecular heat transfer process by calculation of the free-molecule streams between the two plates. In terms of the Knudsen number, the free-molecule thermal conductivity can be written as

$$\lambda_{\text{FM}} = \frac{1}{2}\frac{\alpha_1\alpha_2}{\alpha_1+\alpha_2-\alpha_1\alpha_2}\Lambda\frac{(\gamma+1)C_v P}{\sqrt{2\pi RT}}Kn^{-1} \tag{5}$$

The transition regime (TR) is the most complex one. Many researchers have tried to find a formula for description of heat transfer by the gas in the transition regime. Those efforts were limited and, in general, they have not been successful. However, Sherman's principle of interpolation between the two above explained limiting cases (continuum and free-molecule regimes) represents one of the successful attempts;

$$\frac{1}{\lambda_{\text{TR}}} = \frac{1}{\lambda_{\text{CM}}} + \frac{1}{\lambda_{\text{FM}}} \tag{6}$$

which agreed with experimental results [14] and also with recently published computational results by using the direct simulation Monte Carlo (DSMC) method [15].

4 Modeling and Analysis

4.1 Single-Pore Model (Knudsen Effect)

For modeling the thermal conductivity of the filling gas in a porous structure, we start with the transfer of Kennard's two parallel-plate system to a single-pore model, see Fig. 4, by substituting the distance between the plates by the pore diameter in Eq. 5. Equations 4–6 have been evaluated for the single-pore model, filled by nitrogen at 50 °C, and assuming the accommodation coefficient to be equal to unity. The pore size has been varied to obtain a Knudsen number in the range $10^{-4} < Kn < 10^{2}$. The results are plotted in Fig. 5 where the Knudsen effect is clearly shown: Downscaling of the pore size brings an increase in the Knudsen number and a decrease in the gas thermal conductivity. This effect starts by the end of the continuum regime at about $Kn = 10^{-2}$. Sherman's interpolation, Eq. 6, gives a smooth trend in the transition between the two limiting regimes: the continuum and free-molecule regimes, which is reached at about $Kn = 10$.

4.2 Model for the Gas Thermal Conductivity Including Pore-Size Distribution

Only a few porous materials are monodisperse pore systems, e.g., some foams. For such systems we can apply the above mentioned single-pore model for assessment of the gas thermal conductivity. However, most insulation materials represent bi- or even poly-disperse systems, and it is more complicated to estimate the gas thermal conductivity. The pore-size distribution has been presented as a cumulative distribution function (*CDF*) in Fig. 1, and these functions are used for subdivision of the poly-disperse system into (n) narrow sectors, each of them with a constant mean pore size. The latter ones can be considered as (n) monodisperse systems, and we can use the single-pore model for evaluation of the gas thermal conductivity in the corresponding Knudsen-number range of the sector ($Kn_a - Kn_b$).

$$\bar{\lambda}_{\mathrm{gas},i}\Big|_{Kn_a}^{Kn_b} = \lambda_{\mathrm{gas}}(Kn,\alpha)\Big|_{Kn_a}^{Kn_b} \tag{7}$$

Partitioning the porous system into sectors depends mainly on the corresponding Kn-number range. The sector can be wide for large pores, i.e., the continuum regime, whereas in the transition and free-molecule regimes, the gas thermal conductivity

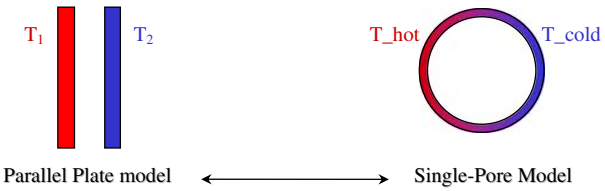

Fig. 4 Sketch of the single-pore model

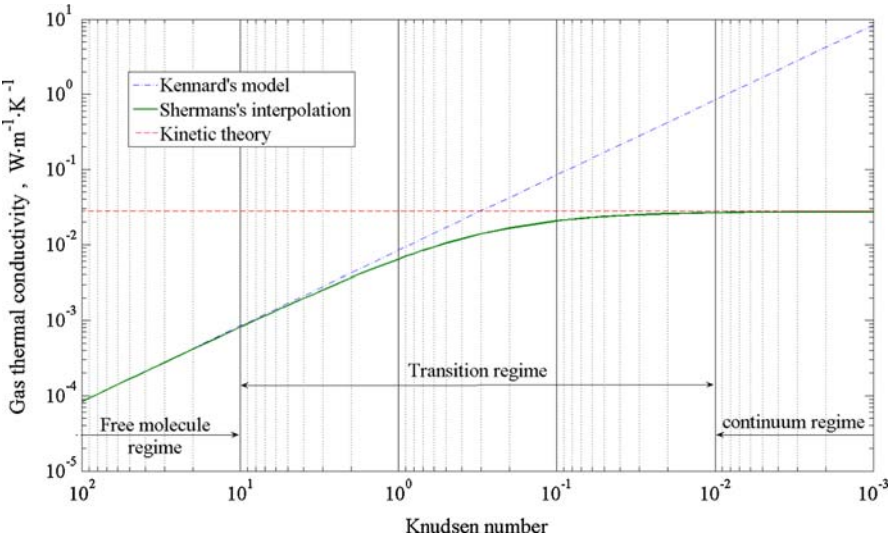

Fig. 5 Evaluation of the single-pore model filled with nitrogen

slides are stronger, as seen in Fig. 5, and therefore the sectors should be narrow to get correct results.

Replacement of the gas atmosphere, e.g., nitrogen by helium, causes a change of the gas thermal conductivity in any sector (i) of the material corresponding to the Knudsen number ($Kn_a - Kn_b$), which is evaluated as follows:

$$\left({}^{N_2}\overrightarrow{\Delta\lambda_{gas}}{}^{He}\right)_i = \bar{\lambda}_{He,i} - \bar{\lambda}_{N_2,i}\Big|_{Kn_a}^{Kn_b} \tag{8}$$

Evaluation of Eq. 8 for two selected materials of each group (a, b, and c in Fig. 1) gives results as presented in Fig. 6 depending on the pore-size distribution. These results reveal that the narrow pore-size distribution, i.e., groups (a) and (b), produce a homogenous apparent gas thermal conductivity along the sample, whereas the wide one, like group (c), gives a different gas thermal conductivity characteristic. In addition, we found for sectors with very small pores, i.e., high Knudsen numbers, that the change in the gas thermal conductivity is very small.

For evaluation of the gas thermal conductivity change in the entire porous system, a model based on parallel arrangement for all sectors can be used:

$$\Delta\lambda_{gas} = \sum_{1}^{n} CDF_i^{i+1} \times \left({}^{gas_1}\overrightarrow{\Delta\lambda_{gas}}{}^{gas_2}\right)_i \tag{9}$$

4.3 Accommodation Effect

By rarefaction of the gas and leaving the continuum regime, molecular collisions with the pore surfaces become more frequent, when compared with inter-molecular col-

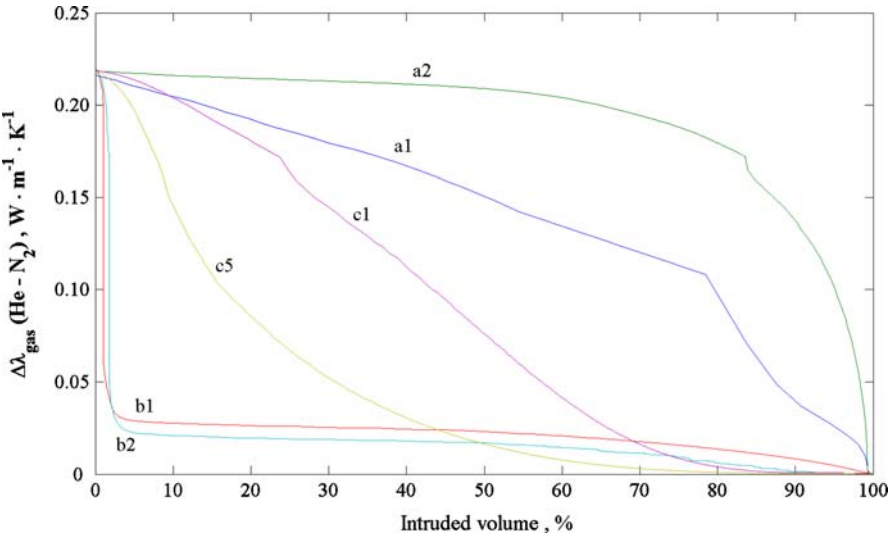

Fig. 6 Effect of exchanging the atmosphere from nitrogen to helium on change of the gas thermal conductivity for six different pore-size distributions

lisions. Subsequently, the accommodation coefficient has an increasing effect on the evaluation of the gas thermal conductivity. This can clearly be seen in Fig. 7, where results from the single-pore model, Eqs. 4 to 6, are plotted versus the Knudsen number. For helium, the accommodation coefficient is decreased from 0.6 to 0.2, and the gas thermal conductivity becomes smaller than that of nitrogen in the range $Kn > 0.3$ whereas the opposite is true for smaller Knudsen numbers. This leaves no doubts that the influence of the accommodation coefficient in the high Knudsen-number regime is large.

4.4 Radiation Effect

To explain the relationship between the radiation and the gas-conduction thermal conductivity, we will consider an exchange of the filling gas inside a single pore, i.e., from low to high gas conductivity. This will cause an increase in the heat conduction between the hot and cold surfaces of the pore, and a new temperature gradient across the pore will be created. It is self-evident that the same effect happens if we have many pores as in porous media. This effect changes the radiation contribution by assessing the effective thermal conductivity of such a porous material. For elimination of changes resulting from the radiation effect, a comparison of the effective thermal conductivities measured in two different gas atmospheres should be carried out at the same temperature levels. The hollow cylindrical arrangement of the sample in our test facility produces a large radial temperature difference, and the measured effective thermal conductivity is actually the average value $\bar{\lambda}_{\text{eff}}$ for the actual temperature difference (T_1, T_2) [16]. By integration of the thermal conductivity over the whole temperature range, the true value of the thermal conductivity can be determined, if the dependence

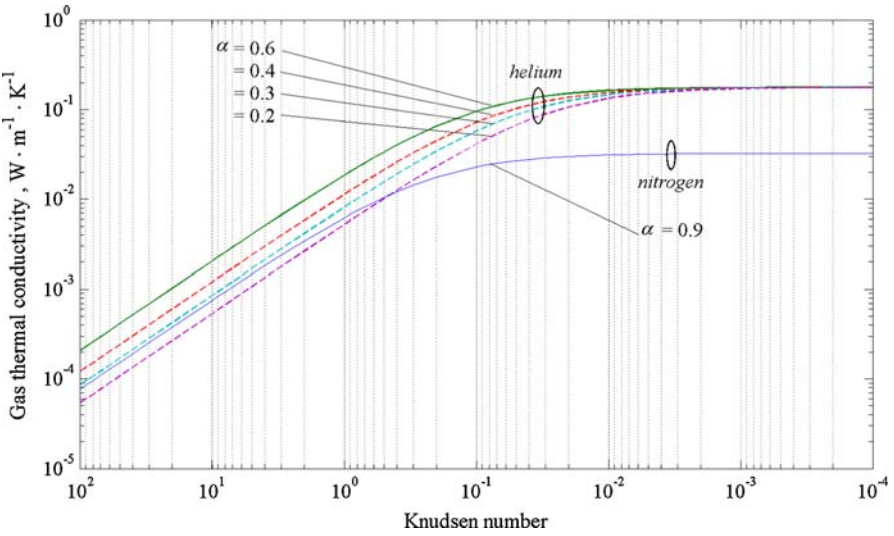

Fig. 7 Influence of the accommodation coefficient in modeling of the gas thermal conductivity by Eqs. 4–6

of the effective thermal conductivity on temperature is known. As several materials with different compositions are considered in this study, it is difficult to formulate the actual temperature influence. Therefore, we assume a polynomial dependence of the third order:

$$\bar{\lambda}_{\text{eff}} = \frac{1}{\Delta T} \int_{T_1}^{T_2} \lambda_{\text{eff,true}}(T) \mathrm{d}T \tag{10}$$

$$\lambda_{\text{eff,true}} = a + bT + cT^2 + dT^3 \tag{11}$$

where a, b, c, and d are constants. By evaluation of Eqs. 10 and 11 at the same temperature levels for two different gases (gas 1 and gas 2), we obtain the change of the effective thermal conductivity due to exchange of the gas atmosphere as

$$^{\text{gas}_1}\overrightarrow{\Delta\lambda_{\text{eff,true}}}^{\text{gas}_2} = \lambda(T, \text{gas}_1)_{\text{eff,true}}\Big|_{T_1}^{T_2} - \lambda(T, \text{gas}_2)_{\text{eff,true}}\Big|_{T_1}^{T_2} \tag{12}$$

4.5 New Correction Model

For prediction of the modification of the effective thermal conductivity we should evaluate the models described by Eqs. 9 and 3. Comparing such results with experimental data evaluated from Eq. 12 gives large deviations, as seen in Fig. 8. The parallel arrangement model Eq. 9 underestimates the change in the effective thermal conductivity of groups (a) and (b) (non-Knudsen materials) and it overestimates that for group (c)

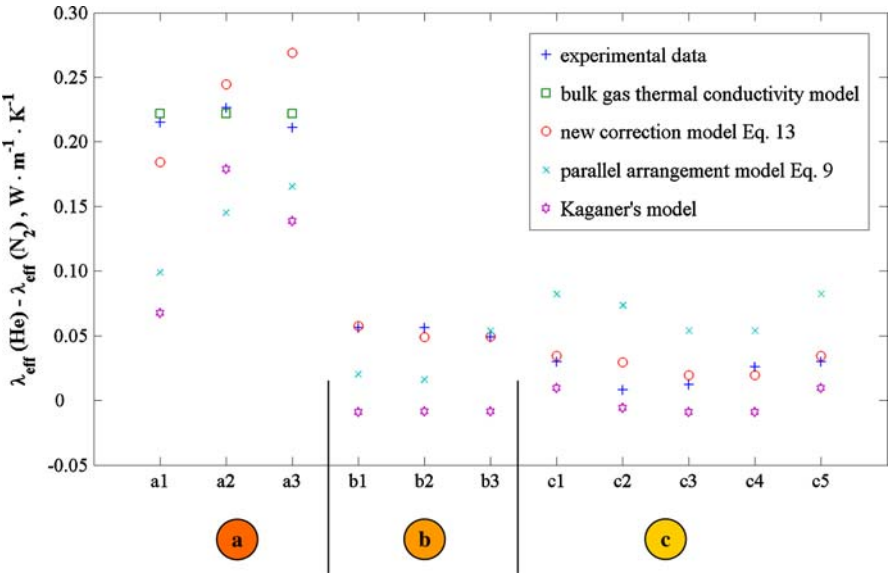

Fig. 8 Results of evaluation of different models and comparison with experimental results

Table 1 Evaluation of exponential parameter for all materials

$\zeta > 1$	Wide distribution, Knudsen materials	$\zeta \cong 1.35$ for all materials in group (c)
$\zeta < 1$	Narrow distribution, non-Knudsen materials	$\zeta \cong 0.73$ for all materials in group (a) and materials (b_1) and (b_2) as well
$\zeta \approx 1$	Wide–narrow distribution, near-Knudsen materials	$\zeta \cong 1.03$ for material (b_3)

(Knudsen materials). This can be interpreted by comparing the effective thermal conductivity of the porous medium with the bulk thermal conductivity of the filling gas, see Fig. 3. This shortcoming can be compensated by a correction based on Eq. 3 as follows:

$$^{\text{gas}_1}\overrightarrow{\Delta\lambda_{\text{eff}}}^{\text{gas}_2} = (\Psi \times \Delta\lambda_{\text{gas}})^{\zeta} \tag{13}$$

with $\Delta\lambda_{\text{gas}}$ evaluated from Eq. 9. The exponential parameter (ζ) reflects mainly two factors: the kind of pore-size distribution (narrow or wide) and the coupling effect between the two phases, namely, gas and solid. A correction between Eq. 3 and the experimental data gave the results as shown in Table 1.

The new correction model (Eq. 13), the parallel arrangement model (Eq. 9), and Kaganer's model have been evaluated for all materials and for the temperature levels ($T_1 = 415\,^{\circ}\text{C}$, $T_2 = 385\,^{\circ}\text{C}$, i.e., at a mean temperature of $400\,^{\circ}\text{C}$). The results are presented in Fig. 8 together with the experimental data.

5 Discussion

The overall results show that only the materials in group (a) are well represented by the bulk gas thermal conductivity model, which gives good agreement with the experimental data, see Fig. 8.

Kaganer's model did not take the pore-size distribution into account, and it is evaluated by using the mean pore size, with the following results: materials in groups (a), (b), and (c) show an underestimation of the thermal conductivity change with the largest deviation for materials (a) with the pore-size distribution extending into the nano-range, see Figs. 1 and 8. As we have seen, the parallel arrangement model of gas thermal conductivity, Eq. 9, gives a good trend estimation of changes in gas thermal conductivity for a poly-disperse porous system. However, deviations in the obtained results from the experimental results could be attributed to two major reasons: the first is the simplification of the conduction model of the two phases, namely, neglecting any coupling between gas and solid; the second is due to the considered parallel arrangement model for the gas thermal conductivities in the various sectors. The new model, Eq. 13, with a well chosen exponential parameter, gives good agreement with the experimental results. Some of the materials, like sample (c_2) show a rather larger deviation compared to others, which actually is due to an increased uncertainty of the measurements for the case of low thermal conductivity. Considering the shape of the pore-size distribution curves (*CDF*), Fig. 1, and the trend of the exponential parameter, Table 1, some general conclusions can be drawn from this model. Estimation of the effective thermal conductivity modification of porous material due to a gas exchange needs basically two types of information: the effective thermal conductivity for one gas atmosphere and the kind of pore-size distribution. With this information the appropriate exponential parameter is chosen and the model, Eq. 13, can be applied.

The strong effects of the accommodation coefficient on the gas thermal conductivity show the importance to have and to develop a measured database for accommodation coefficients of the various insulation materials.

To analyze various porous systems, we can generally use the model of Eq. 9, which gives good understanding of the effect of pore-size distribution on rarefaction of the filling gas in the pores and the follow-up influence on heat transfer through whole systems by exchanging the gas atmosphere. It is found that entire narrow pore-size distribution system always produce a homogenous gas thermal conductivity over the entire structure of the material.

The exchange of the filling gas by a lower thermal conductivity gas in nano-materials does not give a noticeable decrease in the effective thermal conductivity of the materials, especially in the high temperature range. Equations 10–12 can be used to evaluate measured results for obtaining the modification of the effective thermal conductivity due to the change of the thermal conductivity of the filling gas without considering the radiation effect.

6 Conclusion

In the present paper the thermal conductivity of 11 highly porous materials has been investigated by exchanging the filling gas. The results show that the effect of the accom-

modation coefficient increases in the micro- and nano-materials; on the other hand, the lack of experimental data for the accommodation coefficient for the investigated materials produces large problems for independent comparisons between predicted and measured data. Through the determination of the true thermal conductivity of the material, the radiation effect arising from exchanging the filling gas has been eliminated. In modeling of the gas thermal conductivity, more analyses have to be carried out regarding the coupling effect between the gas and solid phases. A new predictive model has been developed covering different effects: pore-size distribution, accommodation coefficient, radiation effects, and coupling effects. The model illustrates the pore-size distribution effect on the effective thermal conductivity, and, based on the kind of CDF, the modification of the effective thermal conductivity by an exchange of the gas atmosphere is well estimated.

References

1. K. Raed, R. Wulf, G. Barth, U. Gross, presented at The seventeenth European conference on thermophysical properties, Bratislava, Slovak Republic (2005)
2. Y.S. Touloukian, P.E. Liley, S.C. Saxena, *Thermal Conductivity Nonmetallic Liquids and Gases, Thermophysical Properties of Matter*, vol. 3 (IFI, New York, 1970), p. 34
3. K. Raed, U. Gross, in *Proceedings of 29th International Thermal Conductivity Conference* (Birmingham, Alabama, USA, 2007), pp. 356–373
4. M.G. Kaganer, *Thermal Insulation in Cryogenic Engineering* (Program for Scientific Translation, Jerusalem, 1969), pp. 6–18
5. G.R. Cunnington, Jr., C.L. Tien, in *Proceedings of 15th International Conference on Thermal Conductivity* (Ottawa, 1977), pp. 325–333
6. J.C. Harper, A.F. El Sahrigi, Ind. Eng. Chem. Fundam. **3**, 318 (1964)
7. Kh. Madzhidov, J. Eng. Phys. Thermophys. **69**, 234 (1996)
8. E.G. Keshock, J. Spacecr. **11**, 41 (1974)
9. S.Q. Zeng, A. Hunt, R. Greif, Trans. ASME **117**, 758 (1995)
10. S.Q. Zeng, A.J. Hunt, W. Cao, R. Grief, Trans. ASME **116**, 756 (1994)
11. K.D Maglic, A. Cezairliyan, V.E. Peletsky, *Compendium of Thermophysical Property Measurement Methods*, vol. 1 (Plenum Press, New York and London, 1984), pp. 63–67
12. C.L. Tien, G.R. Cunnington, Adv. Heat Transfer **9**, 349 (1973)
13. E.H. Kennard, *Kinetic Theory of Gases* (McGraw-Hill, New York and London, 1938), pp. 290–318
14. F.S. Sherman, in *Rarefied Gas Dynamics*, vol. II, ed. by J.A. Lauermann (Academic Press, New York, 1963), pp. 228–260
15. D.J. Rader, W.M. Trott, J.R. Troczynski, M.A. Gallis, J.N. Castaneda, T.W. Grasser, *Microscale Rarefied Gas Dynamics and Surface Interaction for EUVL and MEMS Application* (Sandia National Laboratories, SAND2004-5329, 2004)
16. G. Barth, U. Groß, R. Wulf, Int. J. Thermophys. **28**, 1668 (2007)